A Kinesin-related Protein, KRP_{180}, Positions Prometaphase Spindle Poles during Early Sea Urchin Embryonic Cell Division

Gregory C. Rogers, Kitty K. Chui, Edwin W. Lee, Karen P. Wedaman, David J. Sharp, Gina Holland, Robert L. Morris, and Jonathan M. Scholey

Section of Molecular and Cellular Biology, University of California at Davis, Davis, California 95616

Abstract. We have investigated the intracellular roles of an Xklp2-related kinesin motor, KRP_{180}, in positioning spindle poles during early sea urchin embryonic cell division using quantitative, real-time analysis. Immunolocalization reveals that KRP_{180} concentrates on microtubules in the central spindle, but is absent from centrosomes. Microinjection of inhibitory antibodies and dominant negative constructs suggest that KRP_{180} is not required for the initial separation of spindle poles, but instead functions to transiently position spindle poles specifically during prometaphase.

Key words: Xklp2 • kinesin • sea urchin • mitosis • γ-tubulin

Introduction

During mitosis, the mitotic spindle uses microtubules (MTs)[1] and motors to segregate sister chromatids and to establish the position of the cleavage plane. These events depend upon the accurate positioning of spindle poles during spindle assembly, maintenance, and elongation, and current work is aimed at determining the precise functions of mitotic motors in spindle pole positioning (Hoyt and Geiser, 1996; Sharp et al., 2000).

We have used cleavage stage echinoderm embryos to characterize the functions of mitotic motors, including motors that are involved in spindle pole positioning. The living echinoderm embryo is a classic developmental system for studies of mitosis and cell division as it offers excellent cytology and is amenable to micromanipulation (Wright et al., 1993; Morris and Scholey, 1997; Scholey, 1998). Members of two families of MT-based motors, the kinesins and dyneins, are known to function in positioning both chromosomes and spindle poles during mitosis in a variety of systems (Goldstein, 1993; Vaisberg et al., 1993; Holzbaur and Vallee, 1994; Vernos and Karsenti, 1995; Echeverri et al., 1996; Karsenti et al., 1996; Starr et al., 1998; Sharp et al., 2000). In sea urchin embryos, experiments including microinjection of pan-kinesin antibodies revealed critical mitotic functions for kinesin-related motors in general (Wright et al., 1993). Furthermore, the microinjection of class-specific antibodies revealed that two kinesin-related protein (KRP) motors, KRP_{110} and KRP_{170}, are required for spindle assembly and function, presumably by acting to position spindle poles (Wright et al., 1993; Chui, K.K., G.C. Rogers, A.M. Kashina, K.P. Wedaman, D.J. Sharp, D.T. Nguyen, and J.M. Scholey, manuscript submitted for publication). Finally, a calmodulin-binding COOH-terminal kinesin, Kinesin-C, is present in the early embryo where it is also suspected to participate in spindle pole positioning, but, so far, its function has not been experimentally tested (Rogers et al., 1999).

The functional inhibition of a number of different mitotic motors that are believed to position spindle poles in several systems results in a strikingly similar terminal phenotype: monoastral spindle formation, characterized by duplicated, but closely spaced, spindle poles surrounded by a MT aster attached distally to chromosomes (Vernos et al., 1995; Kashina et al., 1997; Molina et al., 1997; Sharp et al., 1999). Monoastral spindles can arise by one of two pathways: (a) a failure of duplicated spindle poles to separate during spindle assembly, or (b) a plateward collapse of separated poles due to a failure in maintaining spindle shape. Such a phenotype is observed by perturbing the function of the *Xenopus laevis* kinesin Xklp2 in vitro (Boleti et al., 1996). Xklp2 is a plus end–directed kinesin that localizes to centrosomes throughout the cell cycle, being localized to MT minus ends through its interaction with an accessory protein, TPX2 (targeting protein for Xklp2; Wittmann et al., 1998). Functional inhibition of Xklp2 be-

Address correspondence to Jonathan M. Scholey, Section of Molecular and Cellular Biology, 149 Briggs Hall, University of California at Davis, Davis, CA 95616. Tel.: (530) 752-2271. Fax: (530) 752-7522. E-mail: jmscholey@ucdavis.edu

[1]*Abbreviations used in this paper:* DAPI, 4′-6-diamidino-2-phenylindole; GST, glutathione-*S*-transferase; KRP, kinesin-related protein; MAP, microtubule-associated protein; MTs, microtubules; NEBD, nuclear envelope breakdown; ORF, open reading frame.

fore or after spindle assembly in *Xenopus* egg extracts results in the formation of monoastral spindles (Boleti et al., 1996), leading to the proposal that Xklp2, tethered near the centrosome, moves toward the plus ends of MTs attached to the opposite centrosome, thereby driving the separation of spindle poles during spindle assembly and maintenance.

In this report, we have identified and characterized a homologue of Xklp2, called KRP_{180}, from sea urchin early embryos. Using quantitative, real-time imaging of embryos microinjected with inhibitors of KRP_{180}, we show that this motor plays a critical role in positioning spindle poles during mitosis, specifically at prometaphase. Immunolocalization of KRP_{180} and sea urchin γ-tubulin reveals that this motor is not a component of the centrosome but instead concentrates in the region of the central spindle where it may position spindle poles by generating forces on microtubules that are attached to the poles. This study is the first functional analysis of the mitotic function of a member of the Xklp2 subfamily in a living system.

Materials and Methods

Materials

Strongylocentrotus purpuratus (collected from tidepools on the northern California coast) and *Lytechinus pictus* (Marinus, Inc.) sea urchins were used in this study and maintained as outlined by Morris et al. (1997). General reagents were from Sigma-Aldrich unless otherwise stated.

Cloning Sea Urchin KRP_{180} and γ-Tubulin Isoforms

A PCR screen of a *S. purpuratus* unfertilized egg λ ZAP library (Stratagene) with hyperconserved kinesin motor domain sequences yielded a partial cDNA clone encoding the KRP_{180} motor domain. This clone was used for additional library and PCR screens (Rogers et al., 1999) that identified a total of five different KRP_{180} cDNAs that collectively span the entire 4,392-bp ORF.

A partial cDNA encoding sea urchin γ-tubulin was identified in a nested PCR screen of the egg cDNA library using four degenerate primers to hyperconserved sequences found in higher eukaryotic γ-tubulins (Rogers, 2000). This original clone (c9), encoding SpGamma1, was then used in a library screen and two additional γ-tubulin cDNAs were identified [c1 (1.38 kb) and c3 (0.94 kb)] whose nucleotide sequence were identical to each other but different from c9. These two new clones encode a different γ-tubulin isoform (SpGamma2); c1 encodes the entire SpGamma2 ORF. Sequence analysis and structural predictions were performed using the GCG sequence analysis software (Devereux et al., 1984) unless otherwise stated.

Recombinant Proteins and Antibody Production

Two expression plasmids for a GST fusion with the KRP_{180} NH_2-terminal stalk region (named GST-Coil 1) and COOH terminus (named GST-Coil 2) were made by directionally subcloning KRP_{180} nucleotides 1,191–1,965 and 3,495–4,389 into pGEX-GST (Amersham Pharmacia Biotech). *E.coli*–expressed GST-Coil 2 was purified under nondenaturing conditions on glutathione-agarose (Amersham Pharmacia Biotech) and then injected into four female BALB/c mice. After an adequate immune response was reached, polyclonal ascites formation was induced by injection of T-180 sarcoma cells (ATCC) intraperitoneally. Four different batches of ascites fluid from the four mice are identified as polyclonal antibodies 180.1, 180.2, 180.3, and 180.4.

A full-length SpGamma2 cDNA was PCR amplified, subcloned directionally into a pGEX-GST expression plasmid, and expressed/purified under nondenaturing conditions as described for GST-Coil 2. Anti-human γ-tubulin peptide antibody (catalog no. T3559; Sigma-Aldrich) was affinity-purified against recombinant GST-SpGamma2 protein.

Polyclonal antibodies from the anti-KRP_{180} (180.1-180.4) and T3559 sera/crude IgG were affinity-purified against Affigel (Bio-Rad Laboratories) columns precoupled to their respective antigens (GST-Coil 2 and GST-SpGamma2 protein). All affinity-purified antibodies were acid eluted, neutralized in Tris buffer, dialyzed into either microinjection buffer (MIB: 150 mM K-aspartate and 10 mM K-phosphate, pH7.2) or TBS, and concentrated.

Hydrodynamic Studies of KRP_{180}

Native KRP_{180} was partially purified from *S. purpuratus* egg cytosolic extract by a cycle of binding to, and subsequent low salt/ATP elution from, endogenous taxol-stabilized MTs (see Chui, K.K., G.C. Rogers, A.M. Kashina, K.P. Wedaman, D.J. Sharp, D.T. Nguyen, and J.M. Scholey, manuscript submitted for publication). To determine the Stokes radius and sedimentation coefficient of KRP_{180}, MT elution fractions were evenly divided and placed over a gel filtration column or on linear 5–20% sucrose density gradients and all subsequent fractions screened for KRP_{180} by Western blot. The native molecular mass of KRP_{180} was calculated by the method of Siegel and Monty (1966) with the partial specific volume adjusted to 0.716 (Zamyatnin, 1972).

Immunofluorescence Microscopy

Fixation and pre-extraction of sea urchin embryos were performed as previously described (Henson et al., 1995). In brief, dejellied eggs were washed in filtered natural sea water (FNSW) containing 10 mM PABA, fertilized, and monitored with a dissection microscope until first cleavage. Fertilization envelope stripped embryos were fixed with 100% methanol (−20°C), rehydrated stepwise into methanol solutions of TBS + 0.05% Tween (TBST), and blocked with 5% normal goat serum (NGS).

Pre-extraction of mitotic embryos was performed using either 1% NP-40 or 1% Triton X-100 detergent for either 10 or 15 min. Affinity-purified anti-KRP_{180} antibody was used at 1 μg/ml in TBST + 5% NGS. Two different anti–α/β-tubulin antibodies were used: an anti-bovine brain tubulin (Gelfand lab) and an FITC-conjugated anti–α-tubulin monoclonal DM1a (Sigma-Aldrich). Double-labeling with the DM1a and anti-KRP_{180} antibodies was performed as described in Rogers (2000). Secondary antibodies were purchased from Jackson ImmunoResearch Lab. Inc. DAPI (1 μg/ml) was added to the embryos and washed extensively before mounting on poly-L-lysine–coated glass coverslips in a 90% glycerol solution containing 20 mg/ml phenylenediamine in PBS. Indirect immunofluorescent micrographs were obtained as either single optical sections or projections using a Leica TCS SP confocal with each image resulting from 16–32 averaged scans and analyzed using Adobe Photoshop v5.0.

Antibody and Recombinant Protein Microinjection

Control mouse IgG or the four pooled anti-KRP_{180} polyclonal antibodies (180.1–180.4), were dialyzed into MIB and concentrated to 12.4 mg/ml (final intracellular [Ab] at 0.62 mg/ml). Glutathione–Sepharose-purified recombinant GST, GST-Coil 1, and GST-Coil 2 protein was purified in MIB buffer, concentrated, and microinjected at a range of concentrations (final intracellular [protein] from 0.96–9.1 μM). We observed an identical consistent phenotype after introducing GST-Coil 2 protein into early embryos regardless of the protein concentration used, suggesting that the lowest concentration of 0.96 μM was sufficient to inhibit KRP_{180} function. Embryo microinjections were performed by a procedure modified from Kiehart (1982) and Wright et al. (1993). Lateral injection chambers (Kiehart, 1982) allowed high-resolution observation of injections and development by restraining the embryos during cleavage until the ciliated blastula stage. Fertilized eggs were injected with 5% cell volume between 20 min after fertilization until cytokinesis of first cleavage. Embryos were observed by differential interference contrast microscopy on an inverted microscope (model IM-35; Carl Zeiss, Inc.) using a Plan 40× objective and imaged as described (Wright et al., 1993; Morris and Scholey, 1997). An Argus 10 Image Processor (Hamamatsu Photonics) was used for contrast enhancement.

Quantitation of spindle pole positioning and morphology was performed by capturing video printouts of injected embryos, using a Sony UP-880 video graphic printer, every 0.5–5 min at the time of nuclear envelope breakdown (NEBD) or after injection if a spindle was already present. Video prints were digitized using a flatbed scanner and processed using Adobe Photoshop v5.0 and NIH Image v1.62. Spindle pole-to-pole distances were measured as the distance between the center-points of each spindle pole. Changes in these movements over time were plotted using Cricket Graph v1.3.2.

Results

Molecular Analysis of KRP$_{180}$, a Member of the Xklp2 Kinesin Subfamily

We initiated a PCR screen of an unfertilized sea urchin egg cDNA library that was designed to amplify motor domain-specific cDNAs encoding KRPs potentially involved in positioning centrosomes during sea urchin cleavage (Rogers et al., 1999). One of the KRPs obtained in this screen was cloned and sequenced using the strategy outlined in the Materials and Methods. We have named this motor KRP$_{180}$ based on its apparent molecular mass (180 kD) as measured by Western blot of the native protein from sea urchin eggs.

The deduced primary sequence of KRP$_{180}$ predicts a polypeptide 1,463 amino acids in length and a molecular mass of 166,590 Daltons (Fig. 1 A), with an NH_2-terminal motor domain (amino acid residues 1–347) linked to an extensive segment of predicted α-helical coiled-coil, 106 nm long (residues 362-1463; Fig. 1 C). The presence of two predicted PEST sequences (at residues 393–426 and 709–742 with PEST scores +13.22 and 7.56, respectively) sug-

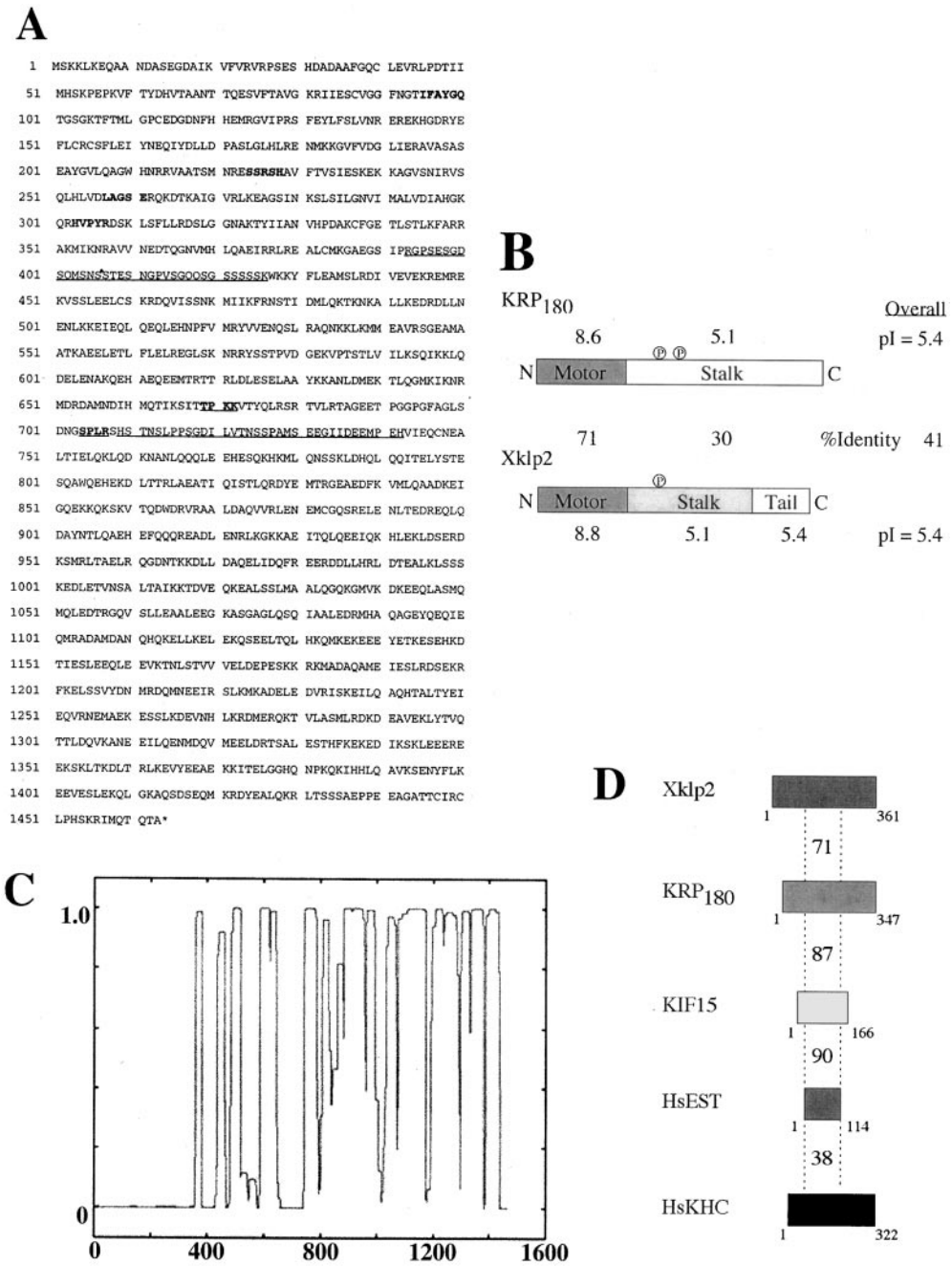

Figure 1. Molecular analysis of sea urchin KRP$_{180}$. (A) The deduced amino acid sequence of KRP$_{180}$ encodes an NH_2-terminal motor polypeptide 1,463 amino acid residues long. Amino acids in bold correspond to the hyperconserved motor sequences found in kinesin motor domains. PEST sequences are shown as underscored amino acids. Underscored and bold amino acids correspond to consensus p34^{cdc2} kinase phosphorylation sites. The nucleotide sequence of KRP$_{180}$ is available from GenBank under accession number AF28433. (B) Aligned linear maps of the motor polypeptides KRP$_{180}$ and Xklp2 demonstrate the conservation of sequence identity and isoelectric point values in their domain organization. Consensus p34^{cdc2} kinase phosphorylation sites are shown as a circled letter P. Sequence identity scores are shown as percentages between the linear maps, isoelectric point values are shown above and below the linear maps, and overall scores are shown on the right. (C) KRP$_{180}$ forms an extensive region of α-helical coiled-coil as determined in a Lupus plot using the Coils program (Lupus et al., 1991). (D) Linear maps of the full-length and partial motor domains of the Xklp2 members found in *Xenopus* (Xklp2), sea urchin (KRP$_{180}$), mouse (KIF15), and human (HsEST), as well as the motor domain of human conventional kinesin heavy chain (HsKHC) demonstrate a region in the catalytic core of the motors, equal to the size of the smallest of the motors shown (HsEST), share identity to the Xklp2 motor domain. Identity scores compared with Xklp2 are shown above each motor domain.

gests that this protein is a target for proteolysis and rapid turnover (Rogers et al., 1986). In addition, two $p34^{cdc2}$ kinase phosphorylation sites [(T/S)PX(K/R); Nigg, 1993; Fig. 1 A], and a predicted tyrosine kinase phosphorylation site (residues 1,135–1141) were found in the stalk region.

KRP_{180} displays a strikingly high degree of homology (71% identity) with the motor of the NH_2-terminal plus end–directed *Xenopus laevis* kinesin, Xklp2, which decreases to 30% outside their motor domains. KRP_{180} and Xklp2 are predicted to form coiled-coil rods that extend throughout the length of their non-motor domains, and they both lack a predicted tail domain, much like class II myosins (Warrick and Spudich, 1987). Both motors share similar $p34^{cdc2}$ kinase consensus phosphorylation sites within their stalk domains that exactly align (Fig. 1 B), suggesting a conserved method of regulation. Finally, we note that Xklp2 homologues have been found in mouse and human (Nakagawa et al., 1997) suggesting that KRP_{180} is a member of a phylogenetically diverse subfamily of kinesins, the Xklp2 subfamily (Fig. 1 D).

Native KRP_{180} from Sea Urchin Eggs Is a Homodimer

To determine the hydrodynamic properties and subunit composition of native KRP_{180}, we raised four mouse polyclonal antibodies against a region of the motor's COOH terminus fused to GST (Fig. 2, lane GST-Coil 2). All four affinity-purified antibodies (180.1–180.4) specifically recognized a 180-kD polypeptide in unfertilized sea urchin egg extract (Fig. 2). Native KRP_{180} was partially purified from egg extract by a single cycle of AMP-PNP–induced binding to endogenous MTs and subsequent release with ATP in either a high or low salt buffer. This eluate was further fractionated by gel filtration and sucrose density gradient centrifugation to measure the hydrodynamic properties of KRP_{180} (Table I). KRP_{180} behaves as a homogeneous protein throughout the biochemical fractionation steps and has a Stokes radius (R_S) of 10.07 nm and a sedimentation coefficient of 8.33 S. (Although, in high salt KRP_{180} displays a sedimentation coefficient of 5.8 S, suggesting that it exists in a folded conformation in low salt that then assumes an elongated conformation in high salt.) Based on these hydrodynamic properties, native KRP_{180} is calculated to have a molecular mass of 334 kD and an axial ratio of 20–40, indicative of a long rod-shaped molecule. Since the deduced mol wt of the cDNA-encoded polypeptide is 167 kD, we predict the native KRP_{180} quaternary structure to be a homodimer lacking any accessory proteins.

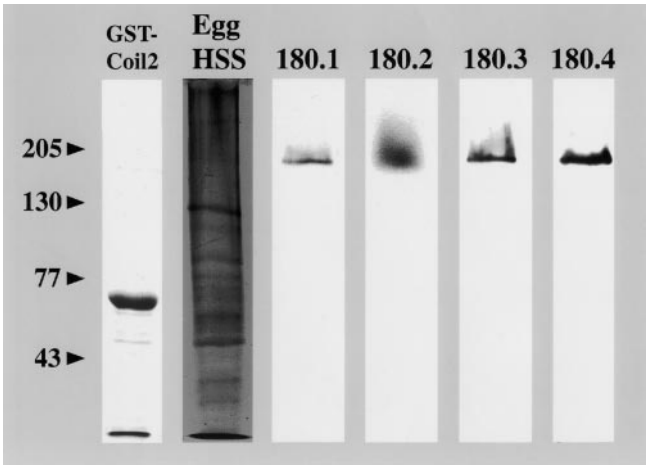

Figure 2. Anti-KRP_{180} antibodies specifically recognize this motor in sea urchin egg extracts. A recombinant GST-KRP_{180} COOH-terminal coiled-coil fusion protein was purified on a glutathione–Sepharose column (lane GST-Coil 2) and used to raise mouse polyclonal antisera. The fusion protein runs at 60 kD. Affinity-purified anti-KRP_{180} antibodies from four different mice all specifically recognize a polypeptide ~180 kD in mass (lanes 180.1, 180.2, 180.3, and 180.4) found in sea urchin high speed supernatant (HSS) unfertilized egg extract (lane Egg HSS; Coomassie-stained SDS-7.5% PAGE).

KRP_{180} Is Concentrated on Microtubules in the Central Region of the Spindle

To determine the intracellular localization of KRP_{180}, we immunolocalized this motor in first cleavage stage *S. purpuratus* whole embryos. During interphase, KRP_{180} localized along astral MT arrays (data not shown) and also displayed a random punctate staining in the cytoplasm during all stages of the cell cycle (Fig. 3, A, E, I, M, and Q). During prophase, KRP_{180} decorated spindle poles in a punctate staining pattern that persisted throughout the completion of mitosis, as well as along MTs that extended around the nuclear envelope (Fig. 3, A–D). In prometaphase, KRP_{180} was concentrated in a filamentous pattern along spindle MTs that invaded the nuclear region (Fig. 3, E–H). KRP_{180} also localized to spindle MTs in metaphase embryos where it appeared asymmetrically distributed, concentrating on the distal ends of half spindle MTs, often as a filamentous pattern crossing the metaphase plate between the chromosomes (Fig. 3, I–L). During anaphase/telophase, KRP_{180} was enriched in the spindle midzone/midbody along MTs bridging the half spindles in this region (Fig. 3, M–T). All anti-KRP_{180} antibodies consistently gave identical staining patterns that were abolished by co-incubation with the antigenic GST-Coil 2 protein (data not shown).

The *Xenopus* Xklp2 motor is unique in its localization in that it concentrates on centrosomes throughout the cell cycle (Boleti et al., 1996); more specifically to MT minus ends in a variety of in vitro structures with or without centrosomes (Wittmann et al., 1998). Although KRP_{180} staining was enriched in the central spindle, a weaker punctate staining pattern on spindle poles was observed. To more clearly determine whether KRP_{180} localized to centrosomes, we obtained an antibody against γ-tubulin, a well characterized component of the centrosome.

Table I. KRP_{180} Hydrodynamic Properties

Property	Low salt	High salt
Stokes radius (R_s)	10.07 nm	–
S value	8.33 S	5.8 S
Native mol wt	334 kD	
Axial ratio	20–40	
Rod length	106 nm	
Estimated mol wt from DNA	167 kD	
Predicted structure	2 × 167 kD = 334 kD homodimer	

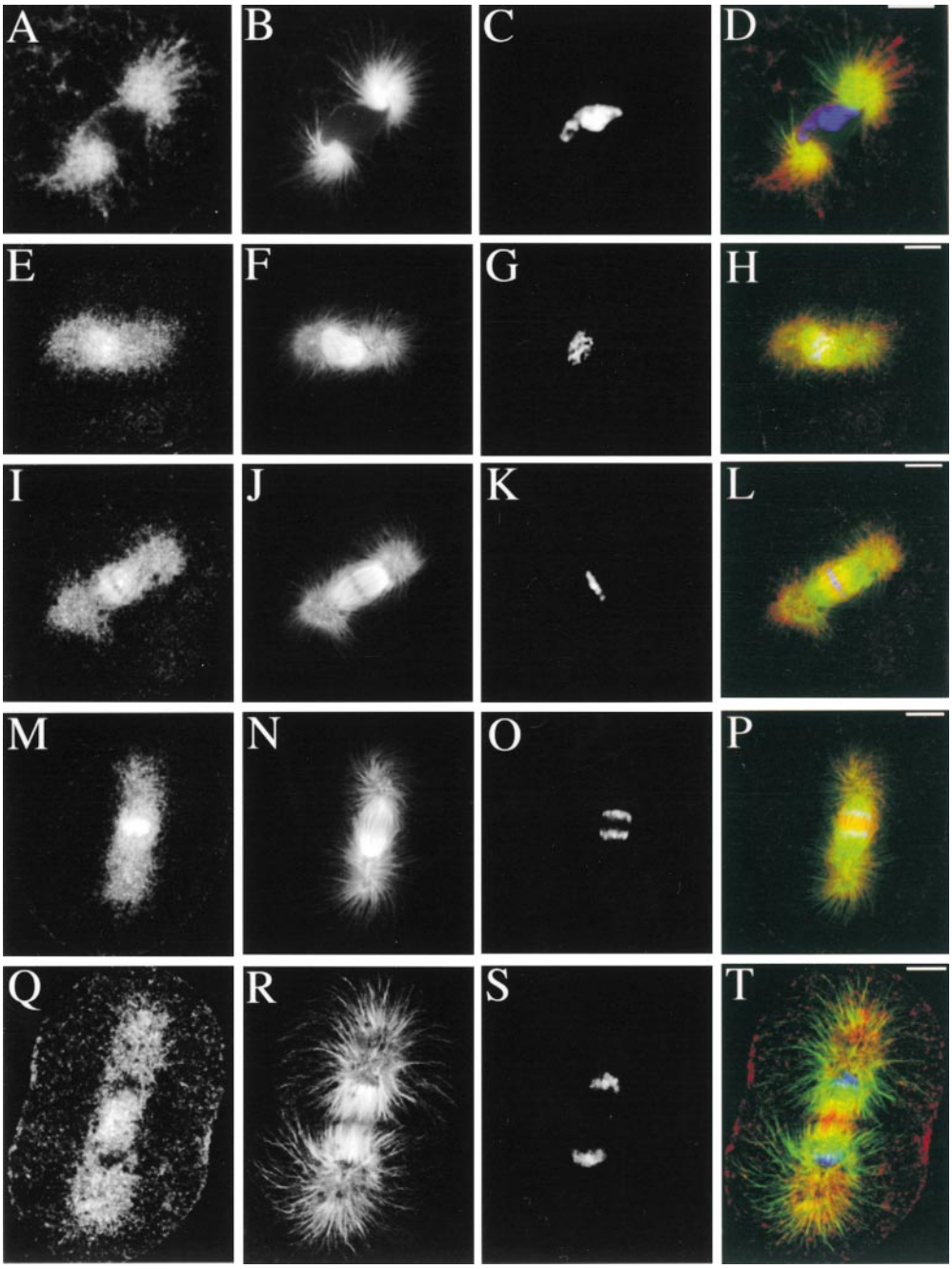

Figure 3. Immunolocalization of KRP_{180} in one-cell cleavage stage sea urchin (*S. purpuratus*) embryos. Whole embryos were methanol-fixed and stained with anti-KRP_{180} (A, E, I, M, and Q) and an FITC-conjugated anti–α-tubulin antibody (B, F, J, N, and R). Anti-KRP_{180} was recognized with Cy5-conjugated secondary antibody and DNA was visualized with (1 μg/ml) DAPI (C, G, K, O, and S). Merged images are shown with KRP_{180} in red, tubulin in green, and DNA in blue (D, H, L, P, and T). Prophase (A–D), prometaphase (E–H), metaphase (I–L), anaphase (M–P), and telophase/cytokinesis (Q–T). Bar, 10 μm.

A PCR screen identified two different isoforms of sea urchin γ-tubulin: a partial cDNA encoding SpGamma1 and a full-length cDNA encoding SpGamma2 (Fig. 4 A). Both γ-tubulin isoforms share significant overall identity (72–89%) with *Drosophila melanogaster*, *Xenopus*, and human γ-tubulins (Fig. 4, A and B). We obtained a commercial anti–γ-tubulin antibody, T3559, because its peptide antigen (residues 38–53 of human γ-tubulin) differed from a sequence found in SpGamma2 by only two conservative substitutions (both Glu to Asp; Fig. 4 A). After affinity-purification against recombinant GST-SpGamma2 (Fig. 4 C, lane 1), the T3559 antibody specifically recognized a single polypeptide in egg high speed supernatant (HSS) that we assumed to be either one or more maternally loaded γ-tubulins (Fig. 4 C, lane 2), as well as recombinant GST-SpGamma2 (Fig. 4 C, lane 3). In addition, T3559 antibody stained centrosomes in pre-extracted mitotic embryos (Fig. 4 D). Pre-extraction of one-cell stage metaphase embryos did not affect the bright filamentous staining of KRP_{180} that colocalized with MTs in the central region of the spindle between the aligned chromosomes (Fig. 5, A–D). However, pre-extraction significantly diminished the punctate staining of KRP_{180} on the spindle poles; longer periods of pre-extraction eliminated nearly all pole staining (Fig. 5, E–H). In embryos that were pre-extracted for an amount of time where the motor was still associated with the poles, KRP_{180} did not colocalize with γ-tubulin at the centrosome (Fig. 5, I–L). The localization of KRP_{180} to the central region of the spindle where MTs are predicted to overlap into antiparallel arrangements

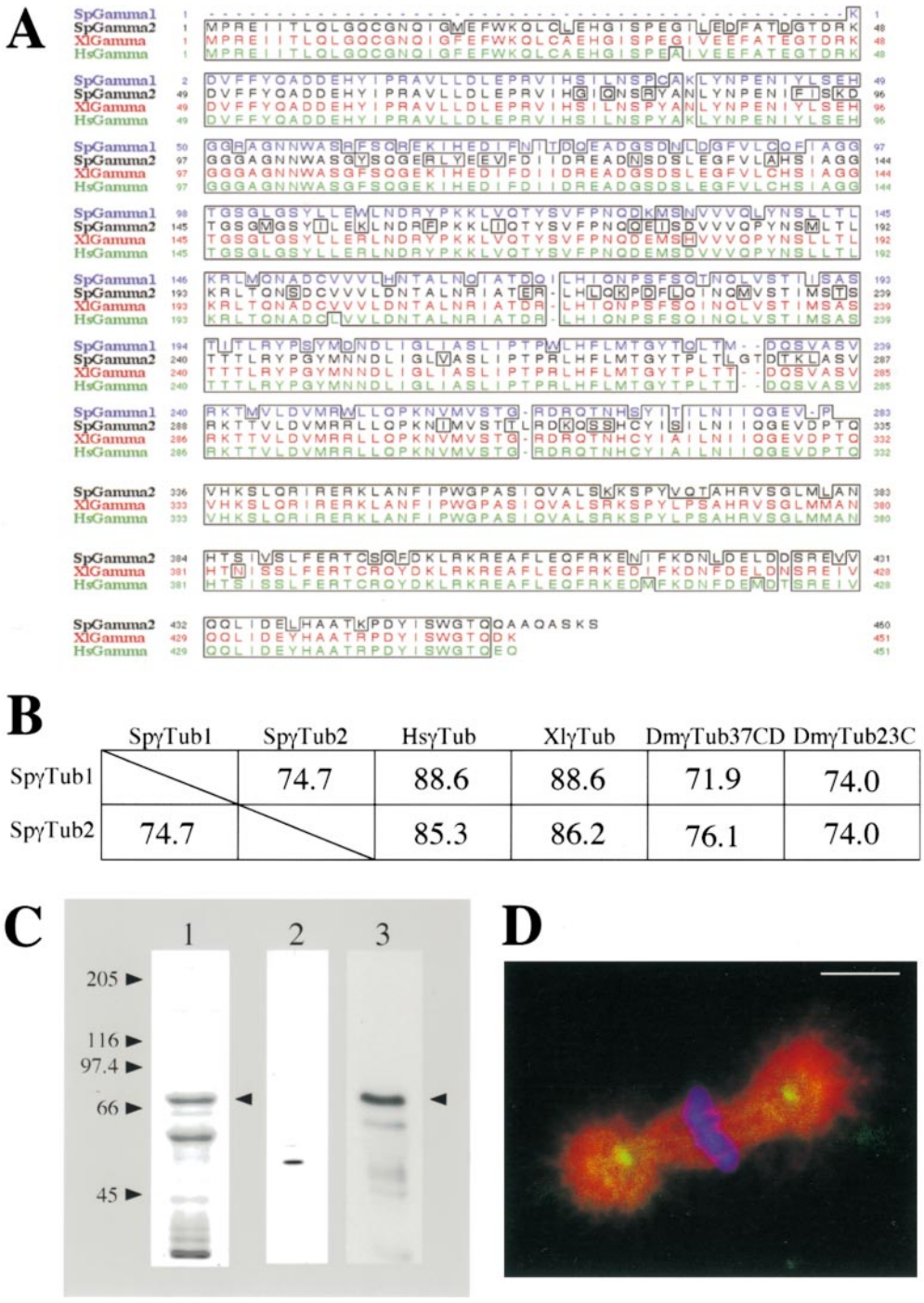

Figure 4. Two different γ-tubulin isoforms (SpGamma1 and SpGamma2) are found in sea urchin (*S. purpuratus*) eggs and early embryos. (A) A lineup of the deduced amino acid sequences of four different γ-tubulins found in sea urchin (SpGamma1 and SpGamma2), *Xenopus* (Xl-Gamma), and human (Hs-Gamma). Identical amino acids between the four γ-tubulins are surrounded with black boxes. The nucleotide sequences of SpGamma1 and 2 are available from GenBank under accession numbers AF284334 and AF284335. (B) Both sea urchin γ-tubulin isoforms (SpγTub1 and SpγTub2) are related to the γ-tubulins found in human (HsγTub), *Xenopus* (XlγTub), and the two isoforms in *Drosophila* (DmγTub37CD and DmγTub23C). The overall percentage of identity that these tubulins share are compared. (C) Purified, recombinant full-length GST-SpGamma2 fusion protein runs at 70 kD upon Coomassie-stained SDS-7.5% PAGE (lane 1). Affinity-purified anti–γ-tubulin antibody specifically recognized γ-tubulin in sea urchin (HSS) egg extract (lane 2) and the SpGamma2 fusion protein (lane 3) by Western blot. The GST-SpGamma2 fusion protein is indicated by the arrowheads and the molecular mass markers correspond to all three lanes. (D) A triple-labeled merged confocal micrograph shows a pre-extracted metaphase sea urchin embryo fixed and stained with anti–γ-tubulin (green), anti–α-tubulin (red) antibodies, and DAPI (blue). Bar, 10 mm.

suggests this motor could crossbridge antiparallel MTs to promote MT-sliding.

KRP_{180} Is Required To Maintain Spindle Shape At Prometaphase, but Not for the Initial Separation of Spindle Poles

To probe KRP_{180}'s function during embryonic cell division, we microinjected affinity-purified anti-KRP_{180} antibodies or control mouse IgG into fertilized sea urchin eggs and observed their effects on spindle pole positioning using quantitative, real-time analysis. The relative movement of spindle poles in control embryos was analyzed by determining the distance between the center points of opposite spindle poles as a function of time (see Fig. 7). One-cell stage embryos microinjected with control nonspecific mouse IgG progressed normally through mitosis and cytokinesis (Fig. 6 A), as well as through subsequent cleavages until ciliogenesis at the blastula stage of development, when observation was terminated (n = 19). Control injected embryos completed mitosis in 40 min on average, from NEBD (time 0) to the completion of cytokinesis

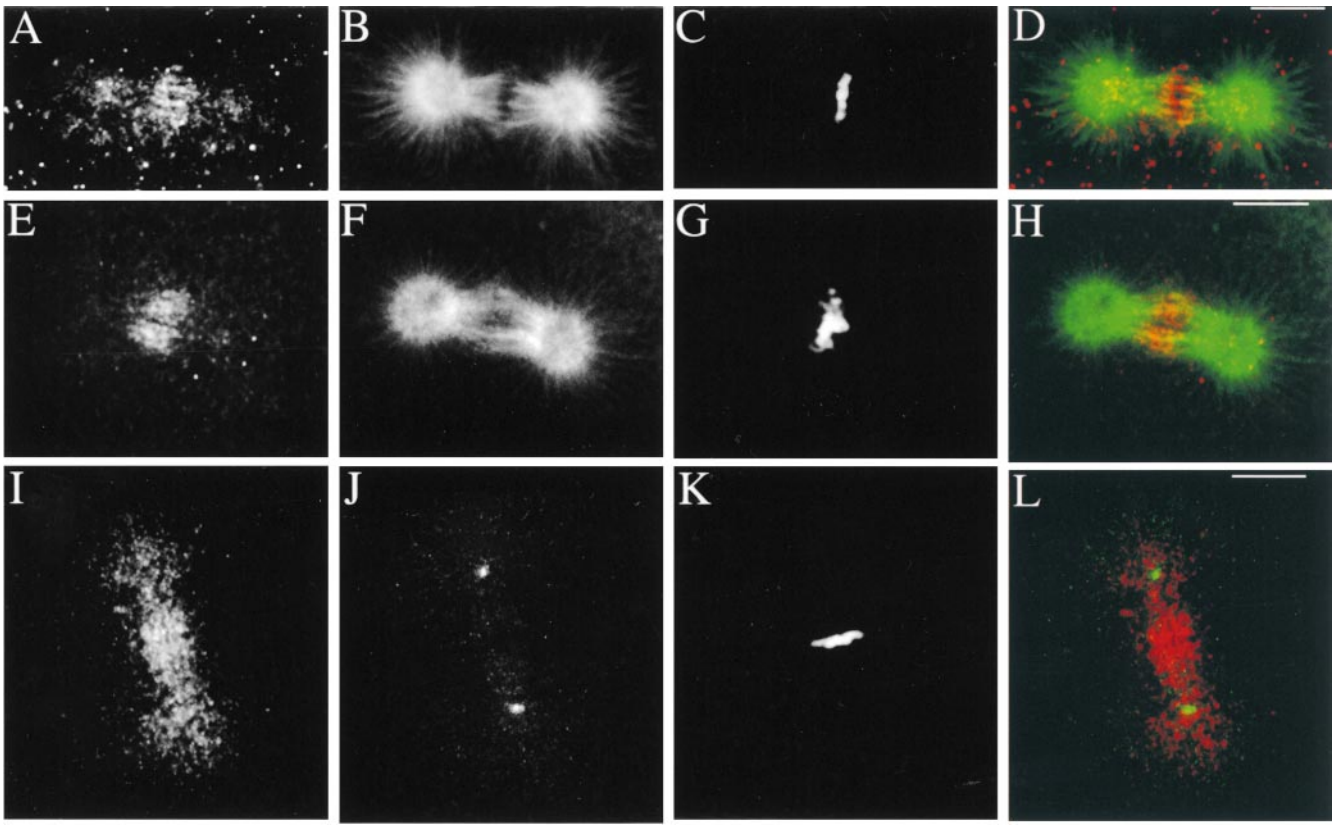

Figure 5. KRP_{180} does not coimmunolocalize to the centrosome with γ-tubulin in one-cell cleavage stage sea urchin (*S. purpuratus*) embryos. Pre-extracted metaphase embryos were fixed and stained with anti-KRP_{180} (A, E, and I) and either an FITC-conjugated anti–α-tubulin antibody (B and F) or an anti–γ-tubulin peptide antibody (J). DNA was visualized with (1 μg/ml) DAPI (C, G, and K). Merged images are shown with KRP_{180} in red and tubulin in green. Bar, 10 μm.

(time, 40 min). As shown in Fig. 7 (open squares), pole separation does not occur at a linear rate, but rather proceeds in a complex fashion. After NEBD, spindle poles maintained a metaphase spacing of ~33 μm for an average of 14.6 ± 4.3 min (n = 6) before initiating anaphase. During anaphase B, these embryos displayed two distinct phases of spindle pole separation: an initial slow phase lasting an average of 12.2 ± 1.9 min (n = 6) and moving at an average rate of 1.08 ± 0.45 μm/min (n = 5) and a fast second phase (8.8 ± 1.7 min [n = 6], 3.55 ± 0.38 μm/min [n = 5]) (Fig. 7; Table II).

We observed an appearance of mitotic defects in anti-KRP_{180} injected embryos that was dependent upon the timing of the injection. Antibody introduced into the embryo during mitosis (i.e., immediately after NEBD) had no effect on the first mitotic division; quantitation of spindle pole separation appeared identical to control embryos (n = 6; data not shown). However, embryos that were injected during interphase displayed one of three distinct phenotypes. (a) Embryos that were delayed in initiating NEBD (50 min on average) and displayed a prophase morphology with separated spindle poles on opposite sides of the nucleus (8 of 18 embryos). (b) Embryos that arrested in the cell cycle in a prophase morphology (6 of 18 embryos). These embryos had arrested for 37 min on average with an intact nucleus and then died. Embryonic cell death is hallmarked by a dynamic ruffling of the cell cortex as the cytoplasm turns granular followed by cell lysis; such behavior is characteristic of apoptosis as proposed by Hinchcliffe et al., 1998. (c) Embryos that displayed no defects or delays before NEBD (4 of 18 embryos).

Of the anti-KRP_{180} antibody containing embryos that were injected in interphase and entered mitosis, all clearly displayed two separated spindle poles positioned on opposite sides of the nucleus before NEBD, suggesting that KRP_{180} is not required for the initial separation of spindle poles at prophase (12 of 12 embryos; categories a and c above). However, all of these embryos underwent a dramatic spindle collapse immediately upon NEBD where separated poles moved plateward at an average rate of 2.0 ± 0.41 μm/min (n = 4; Fig. 6 B; Table II). Measurements of spindle pole separation as a function of time of a representative embryo is shown in Fig. 7. Although the spindle had collapsed, poles were clearly visible in a side-by-side position (Fig. 6 B; 15.32 min) with an average pole-to-pole distance of 20.4 μm ± 0.25 (n = 6). Most collapsed spindles continued into anaphase displaying both slow and fast phases of anaphase B at rates and durations observed in controls (8 of 12 embryos; Fig. 7; Table II). However, 4 of 7 embryos did display subtle defects in the rates and length of time spent in the first slow phase of anaphase B, and slight defects in cytokinesis were observed as well (3 of 8).

In addition to antibody microinjection, we studied this motor's mitotic function by introducing recombinant trun-

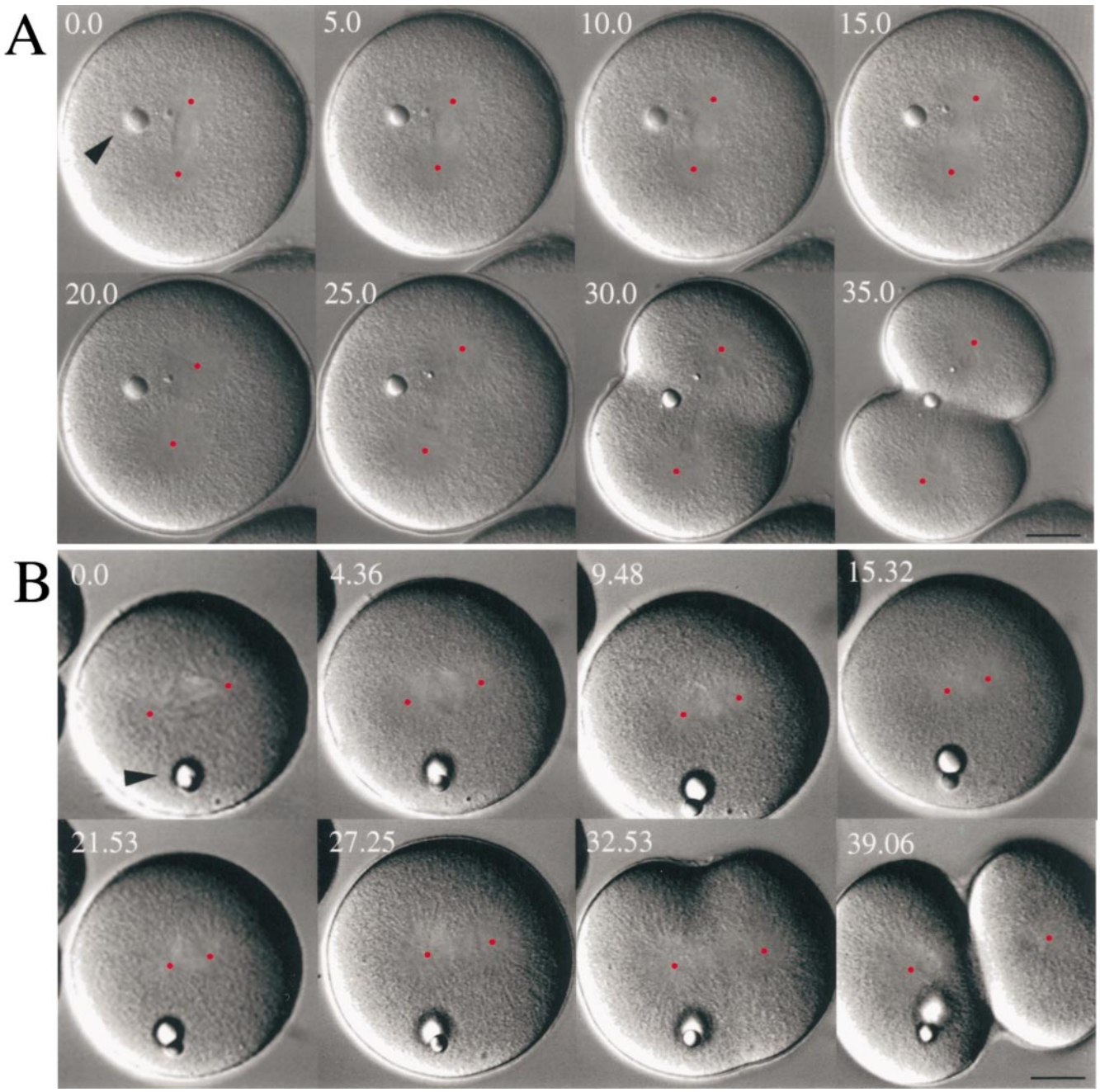

Figure 6. Effects of anti-KRP_{180} and control antibody microinjected into mitotic sea urchin (*L. pictus*) embryos. Video frames of representative control IgG (A) and anti-KRP_{180} (B) injected embryos are shown. The video frames (with time shown as minutes and seconds) show the effects of microinjection on first cleavage in both embryos during NEBD (time 0.0 min) until the completion of cytokinesis (time 35.0 min for control and 39.06 for experimental embryo). Both embryos were microinjected in interphase, shortly after fertilization. The center of each pole is marked with a red dot to assist in measuring spindle pole-to-pole distances. The intracellular oil droplets (arrowheads) confirm that both embryos were microinjected successfully. Bar, 20 μm.

cated KRP_{180} proteins into one-cell stage embryos. Such constructs might act as dominant negative proteins by competing with the endogenous motor complex for binding to cargo or transiently-associated accessory polypeptides. To this end, we designed NH_2- and COOH-terminal GST-tagged coiled-coil encoding constructs designated GST-Coil 1 and GST–Coil 2 (Figs. 8 A and 2). The sequence for the GST-Coil 1 and Coil 2 domains was based on the work of Boleti et al. (1996) who found that GST constructs of the exactly homologous Xklp2 domains functioned as a negative control and as a dominant negative, respectively, in in vitro spindle assembly assays.

We have found that microinjection of GST-Coil 2 into one-cell stage embryos completely phenocopied the results obtained with the antibody injection experiments. As in anti-KRP_{180}–injected embryos, GST-Coil 2 injected embryos displayed mitotic defects dependent upon the timing of the injection. Recombinant protein injected during mi-

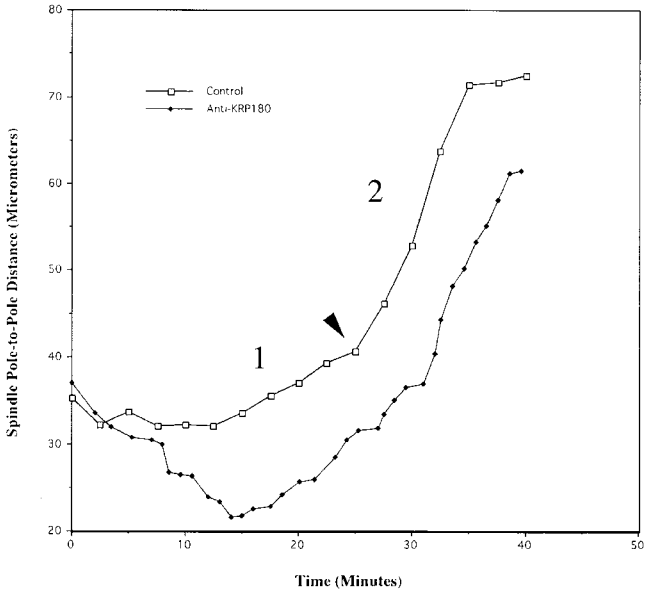

Figure 7. KRP_{180} is required to maintain spindle shape in prometaphase sea urchin embryos. Spindle pole-to-pole distances were measured over time in control and anti-KRP_{180} antibody injected embryos. Time 0 in each graph represents NEBD and the final time point in each graph indicates the completion of cytokinesis. Bold type numbers 1 and 2 indicate two distinct phases of anaphase B spindle elongation. The arrowhead indicates the transition from the first slow phase of spindle pole elongation to the second fast phase.

tosis (i.e., after NEBD) had no effect on the first embryonic cleavage as determined by quantitation of spindle pole separation over time compared with controls ($n = 13$; data not shown). However, every GST-Coil 2 containing embryo that was injected either during interphase ($n = 9$) or immediately at NEBD ($n = 2$), displayed spindle poles on opposite sides of the nucleus that moved plateward after completion of NEBD: a phenotype strikingly similar to anti-KRP_{180} injected embryos. We observed that GST-Coil 2 was a less potent inhibitor of KRP_{180} function as compared with the anti-KRP_{180} antibody because the GST-Coil 2–induced spindle collapse occurred at a rate less than half that observed in anti-KRP_{180} injected embryos (Table II). In addition, the extent of spindle collapse (depicted by the length of the collapsed metaphase spindles) was less in embryos injected with GST-Coil 2 than anti-KRP_{180} (25.1 ± 3.0 μm [$n = 10$] as opposed to 20.4 μm). Measurements of spindle pole separation as a function of time and video frames of a representative GST-Coil 2 injected embryo are shown in Fig. 8, B and C. Mitotic arrest was not observed in embryos whose spindles had collapsed ($n = 11$), and anaphase B was initiated at rates and durations similar to those observed in control injected embryos (Table II). As was observed with the anti-KRP_{180} injections, a small percentage of GST-Coil 2 injected embryos displayed defects in the duration and rate of the initial slow phase of anaphase B (18%) or divided asymmetrically (9%; Fig. 8 C). Finally, as observed in antibody injected embryos, injection of GST-Coil 2 before NEBD resulted in one of three phenotypes: a prophase delay for an average of 40.5 min (2 of 11 embryos), a prophase arrest leading to cell death (2 of 11 embryos), or no defects or delays before NEBD (7 of 11 embryos).

As was found for control IgG injected embryos, microinjection of either GST-Coil 1 ($n = 9$) or control GST protein ($n = 11$) during interphase or mitosis had no deleterious effect on first cleavage embryos. Kinetic analysis of pole-to-pole positioning revealed that GST-Coil 1– and GST-injected embryos maintained average metaphase spindle lengths of 31.8 μm and 30.9 μm, respectively, before initiating anaphase (Fig. 8 B; Table II). Likewise, during anaphase B, these embryos displayed a characteristic biphasic separation of spindle poles: an initial slow phase followed by a fast second phase (Fig. 8 B; Table II).

Thus, the injection of KRP_{180} inhibitors, either antibody or a dominant negative construct, results in the collapse of bipolar spindles. Taken together, these data suggest that KRP_{180} functions to position spindle poles and thus to transiently maintain prometaphase spindle shape in early sea urchin embryos.

Discussion

KRP_{180} and the Xklp2 Subfamily of KRPs

The molecular data on KRP_{180} from sea urchin embryos suggests that this motor protein belongs to a phylogenetically diverse subfamily of KRPs, whose founding member is the centrosome-associated motor, Xklp2 (Boleti et al., 1996), which also has homologues in humans, mice, *Arabi-*

Table II. Spindle Dynamics in Antibody and Recombinant Protein-injected Embryos

	Reagent									
	Mouse IgG	*n*	Anti-KRP_{180}	*n*	GST	*n*	GST-Coil 1	*n*	GST-Coil 2	*n*
Average velocity					*μm/min*					
Rate of slow phase	1.08 ± 0.45	5	1.06 ± 0.06	3	1.41 ± 0.32	4	1.30 ± 0.1	5	1.04 ± 0.38	9
Rate of fast phase	3.55 ± 0.38	5	3.22 ± 0.60	7	3.80 ± 0.75	4	3.90 ± 0.97	5	3.37 ± 0.53	10
Rate of spindle collapse	NA		2.00 ± 0.41	4	NA		NA		0.87 ± 0.2	7
Average time					*min*					
Initiation of anaphase*	14.6 ± 4.3	6	16.0 ± 3.2	6	12.8 ± 4.3	4	13.0 ± 3.5	5	15.2 ± 3.5	8
Duration of slow phase	12.2 ± 1.9	6	10.5 ± 1.3	3	11.4 ± 2.9	4	13.3 ± 3.3	5	12.5 ± 1.9	9
Duration of fast phase	8.8 ± 1.7	6	11.3 ± 4.8	7	7.3 ± 2.5	3	8.3 ± 2.5	4	7.8 ± 1.8	9

NA, Not applicable because this event did not occur.
*Indicates the time (post-NEBD) anaphase B begins.

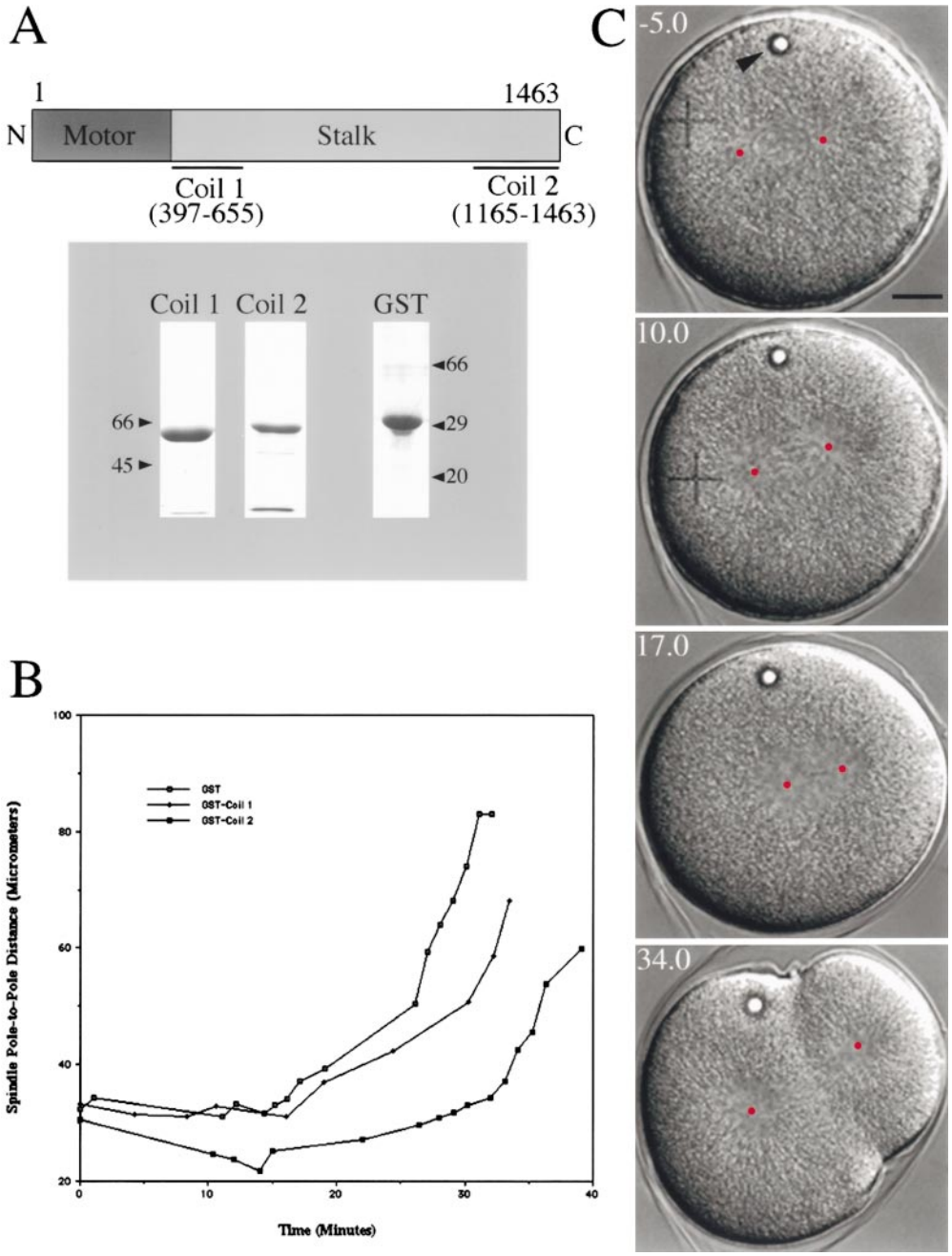

Figure 8. Effects of GST-KRP_{180} dominant/negative protein microinjected into mitotic sea urchin (*L. pictus*) embryos. (A) Purified GST-KRP_{180} stalk fusion proteins (Coil 1 and Coil 2) were used as dominant/negative proteins. The numbers below the linear map of the KRP_{180} polypeptide correspond to the amino acids that comprise the fusion proteins. Molecular mass markers indicate the size of the glutathione–Sepharose-purified fusion proteins (lane Coil 1 and 2; Coomassie-stained 7.5% and lane GST; 12% SDS-PAGE). (B) Microinjection of GST-Coil 2 into mitotic embryos perturbs the maintenance of prometaphase spindle shape, whereas microinjection of GST-Coil 1 and control GST does not. Spindle pole-to-pole distances were measured over time for individual spindles in GST-, Coil 1–, and Coil 2–injected embryos. Time 0 represents NEBD and the final time point indicates the completion of cytokinesis. Anaphase B initiates ~15 min post-NEBD in the three spindles shown. (C) Video frames of a representative GST-Coil 2 injected embryo are shown. The video frames (with time in minutes) show the effects of microinjection on first cleavage five minutes before NEBD (time −5.0) until near the completion of cytokinesis (time 34.0). This embryo was microinjected in interphase, shortly after fertilization. The center of each spindle pole is marked with a red dot to assist in spindle length measurements while the intracellular oil droplet (arrowhead) indicates a successful microinjection. This embryo divides asymmetrically due to mispositioning of the spindle after displaying a prometaphase spindle collapse.

dopsis thailiana and *Oryza sativa* (Nakagawa et al., 1997; Lee, Y.-R., and B. Liu, personal communication). Hydrodynamic data suggest that KRP_{180}, like Xklp2, is a homodimer of two motor subunits (Wittmann et al., 1998). Functional data suggest that sea urchin KRP_{180} serves to position spindle poles during prometaphase in early embryos. Similarly, Xklp2 serves to separate spindle poles in spindle assembly assays using *Xenopus* egg extracts (Boleti et al., 1996). Thus, members of the Xklp2 subfamily of KRPs may have important mitotic roles involving spindle pole positioning in a wide range of systems.

KRP_{180}, a Mitotic Motor Required to Maintain Prometaphase Spindle Shape

Our immunolocalization data suggest that KRP_{180} is localized to interzonal MTs where it could serve to generate forces that position the attached spindle poles during prometaphase. In contrast, Xklp2 concentrates on centrosomes during all cell cycle stages (Boleti et al., 1996). Thus, although both KRP_{180} and Xklp2 are found to position spindle poles, the mechanisms by which they are proposed to do so differ.

Based on its localization to a region of the spindle where MTs overlap in an anti-parallel fashion, it is tempting to hypothesize that KRP_{180} functions to crossbridge anti-parallel MTs and drive MT-sliding. Assuming that KRP_{180} is a plus end–directed motor as was found for Xklp2 (Boleti et al., 1996), it could drive the separation of spindle poles by exerting force on antiparallel spindle MTs to which the poles are attached, as has been suggested with members of the bimC/bipolar kinesin subfamily (Sharp et al., 2000).

Microinjection of sea urchin embryos with KRP_{180}-specific antibodies and recombinant dominant/negative constructs demonstrates that KRP_{180} is required to maintain the separation of spindle poles during first cleavage. Immediately after NEBD, every anti-KRP_{180} and GST-Coil 2 injected embryo we observed underwent a dramatic spindle collapse: poles moved plateward at a linear rate and assumed a juxtaposed position, giving rise to monoastral spindles. Such monoastral spindles are a hallmark of cells that fail to divide. For example, similar structures have been seen after the inhibition of either Xklp2 or Eg5 in *Xenopus* extracts suggesting that both these motors contribute to the formation of bipolar spindles (Sawin et al., 1992; Boleti et al., 1996). However, since the studies in *Xenopus* were performed using fixed images, it was unclear exactly when these motors exert their effects. In contrast, the live cell imaging described here strongly suggests that KRP_{180} serves to generate outward forces on spindle poles specifically after the initial separation of the spindle poles during prometaphase.

Quantitation of spindle pole movements in both anti-KRP_{180} and dominant negative protein injected embryos revealed that most collapsed spindles were able to initiate anaphase and complete mitosis. Occasionally we observed slight defects in spindle elongation and cytokinesis. We attribute these observations to structural defects in the organization of the spindle midzone/midbody on which these events depend, and that perhaps these structures had not assembled properly due to the close proximity of the poles after the spindle collapse. However, due to its midzone/midbody localization, we cannot rule out the possibility that KRP_{180} might function to assemble or promote MT-sliding during late mitosis in a semi-redundant fashion with other mitotic motors as well (see below).

Proposed Model of Mitotic Motor Functions

How is the mitotic function of KRP_{180} integrated into the mitotic function of other motors that operate in the early sea urchin embryo? Assuming that the functional inhibition of KRP_{180} by specific antibody and dominant/negative protein microinjection reveals the full spectrum of this motor's mitotic function, then these results suggest a specific role for KRP_{180} in maintaining prometaphase spindle shape. In addition to KRP_{180}, we have also characterized new sea urchin motors that play important roles in positioning spindle poles during embryonic cleavage. These include the spindle-associated motors, KRP_{110} and KRP_{170} (members of the plus end–directed MKLP1 and bipolar kinesin subfamilies, respectively), a cortically localized cytoplasmic dynein, and a COOH-terminal kinesin, Kinesin-C, that is related to a unique class of Ca^{2+}/calmodulin–regulated motors and whose function is unknown (Chui, K.K., G.C. Rogers, A.M. Kashina, K.P. Wedaman, D.J. Sharp, D.T. Nguyen, and J.M. Scholey, manuscript submitted for publication; Rogers et al., 1999; Rogers, 2000). Functional analysis of $KRP_{110,}$ KRP_{170}, and cortical dynein, by microinjection of antibodies and dominant/negative inhibitors, revealed that perturbation of any one of these three motors results in a prophase cell cycle arrest, implying a role for these motors in the initial assembly of the spindle. Similar studies also demonstrated a metaphase or anaphase cell cycle arrest when KRP_{110} and KRP_{170} function was perturbed, respectively. In addition, both KRP_{170} and cortical dynein are required for specific phases of spindle elongation at anaphase.

We propose that the predominant force driving spindle pole positioning is through the MT-sliding activity of these mitotic motors. Native KRP_{110} and KRP_{170} are homotetramers with a predicted bipolar ultrastructure (i.e., two motor domains on opposite ends of a coiled-coil rod), whereas native KRP_{180} is homodimeric with an extensive 106-nm rod. Interestingly, KRP_{180} has an axial ratio of 20 like KRP_{110}, whereas KRP_{170} has a longer axial ratio of 80. Given the differences in axial ratios, these motors could crossbridge adjacent MTs with varying space between them. For example, adjacent MTs with a long spacing would be cross-linked by KRP_{170} that would then be linked into tight MT bundles by the action of KRP_{110} and KRP_{180}. Such an activity of anti-parallel MT capture and bundling by MT cross-linking motors, combined with their subsequent force generating properties to promote MT sliding, would result not only in the ability to position spindle poles, but to establish the structural integrity of the spindle. Not surprisingly, functional inhibition of these motors results in cell cycle arrest phenotypes, possibly due to direct interference with spindle mechanics. We also propose that minus end–directed, cortical dynein and Kinesin-C function to position spindle poles using a MT-sliding mechanism. COOH-terminal kinesins function to counterbalance the pole separating forces of the bipolar kinesins, whereas dynein slides MTs relative to an actin-rich cortical network to which it localizes (Saunders and Hoyt, 1992; Pidoux et al., 1996; O'Connell et al., 1993; Mountain et al., 1999; Sharp et al., 1999, 2000; Rogers, 2000).

These results suggest a plausible model for the pathway of spindle pole positioning during embryonic cell division through the coordinating functions of five different plus and minus end–directed MT-based motors (Fig. 9). Before NEBD, cortical dynein, KRP_{110}, and KRP_{170} work together to coordinate the initial separation of spindle poles. Pole separation would result from the combined activities of cortical dynein pulling on astral MTs and the homotetrameric (and predicted bipolar) motors, KRP_{110} and KRP_{170}, cross-linking and sliding anti-parallel MTs. KRP_{170}, which has a greater axial ratio than KRP_{110}, would cross-link adjacent anti-parallel spindle MTs with a long spacing that would then be linked into tighter MT bundles by the action of KRP_{110}, serving to stabilize the connections between the poles as they are pushed/pulled around the nucleus.

At prometaphase, separated poles are held apart and spindle shape maintained by KRP_{180} through its putative ability to crossbridge antiparallel MTs of short spacing (via interaction with an unidentified MT-binding acces-

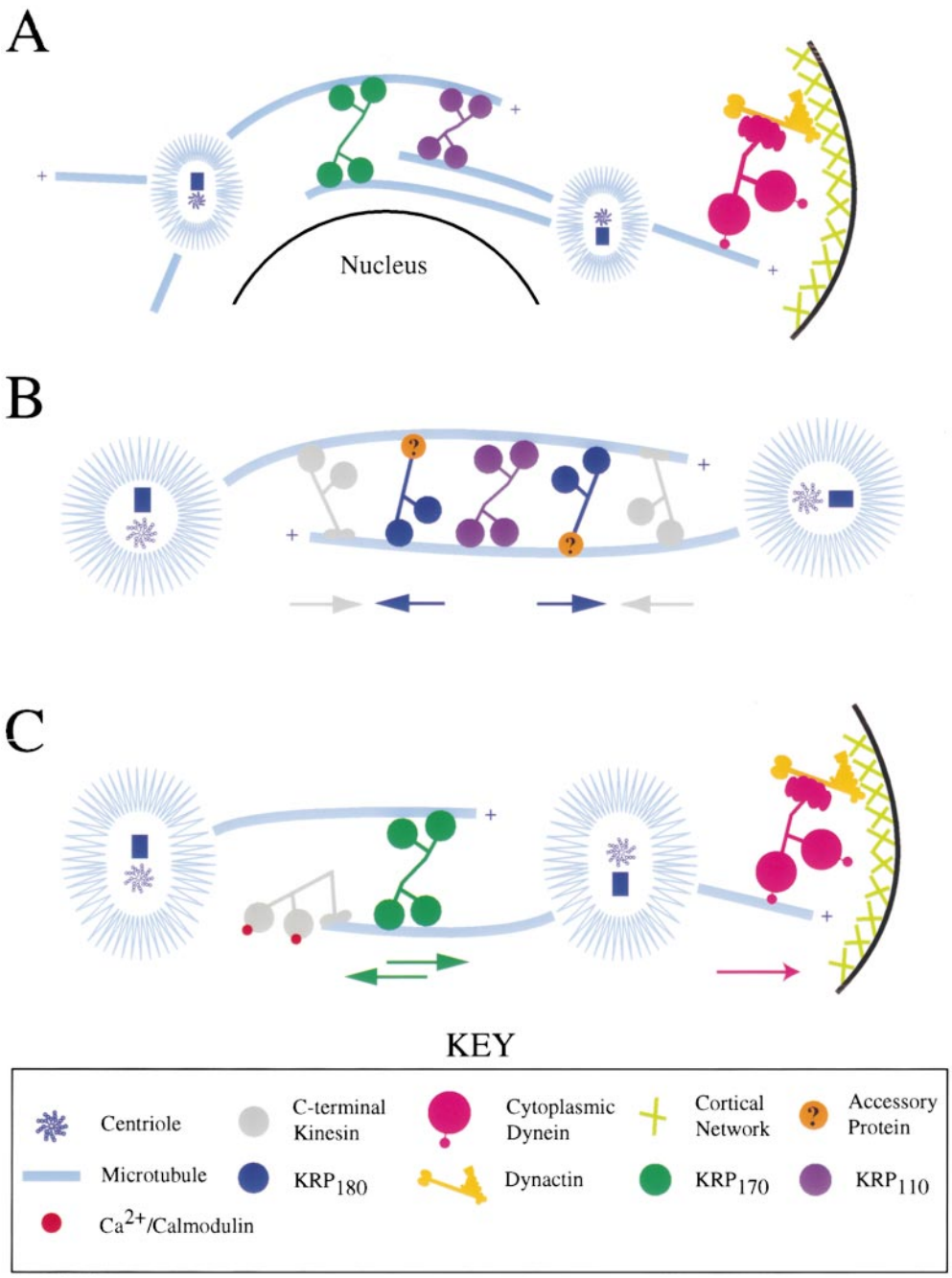

Figure 9. Proposed model describing the pathway of spindle pole positioning during embryonic cell division using the five MT-based motors: KRP_{180}, the COOH-terminal kinesin (Kinesin-C), cytoplasmic dynein, KRP_{110}, and KRP_{170}. Diagrams are shown for the proposed timing and mechanisms of action during (A) prophase/spindle assembly, (B) (pro)metaphase/spindle maintenance, and (C) anaphase B/spindle elongation. Colored arrows indicate the direction of force exerted by the motor of the same color.

sory protein) and to slide MTs (and poles) apart. KRP_{180}'s poleward force would be counterbalanced by a plateward force, attributed to Kinesin-C (Fig. 9 B). Collapse of the spindle in the absence of KRP_{180} function, although not always lethal, would decrease the fidelity of later mitotic events such as proper spindle elongation and cytokinesis, due to the inability of subsequent MT structures to form properly in the central spindle. In addition, KRP_{110} would also cross-link spindle MTs into tight bundles to enhance the integrity of the spindle.

Spindle elongation could be triggered by the inactivation of Kinesin-C. Plant homologues of Kinesin-C are inactivated when their motor domains bind Ca^{2+}/calmodulin (Song et al., 1997). In sea urchin embryos, $[Ca^{2+}]_i$ drops after NEBD and then rises globally at the metaphase-anaphase transition (Groigno and Whitaker, 1998). In our model, Kinesin-C motor activity is turned on after NEBD when it would crossbridge MTs and maintain spindle shape by exerting a plateward force on the poles throughout (pro)metaphase. When $[Ca^{2+}]_i$ increases at the beginning of anaphase, Kinesin-C is turned-off, releasing the plateward force on the spindle poles and allowing spindle elongation to occur in two extensive phases driven by the MT-MT sliding bipolar kinesin, KRP_{170}, and cortical dynein pulling on astral MTs (Fig. 9 C). Additional studies performed in echinoderm embryos (Scholey, 1998) combined with complementary studies performed in organisms amenable to genetic manipulation (Sharp et al., 2000)

will be required to test this model and elucidate the precise roles that multiple mitotic motors play in spindle pole positioning.

In conclusion, the data described in this paper identify KRP_{180} as a member of the Xklp2 subfamily of mitotic motors and provide the first evidence of this motor's activity in vivo. A combination of function-blocking reagents was used to show that KRP_{180} serves to position spindle poles specifically during prometaphase. The notion that this motor functions during such a specific phase of mitosis underscores the subtle roles that some mitotic motors may perform in spindle function.

We would like to thank all of the members of the Scholey Lab and especially Drs. Daniel Buster, Stephen Rogers, Frank McNally, Lesilee Rose, and Bo Liu for helpful scientific discussions and critical reading of the manuscript. We would also like to thank Dr. Heiner Matthies for technical help with bacterial expression and discussions. Also, we thank the Gelfand lab for the anti-tubulin antibody.

This work was supported by a grant from the National Institutes of Health no. GM55507 to J.M. Scholey.

Submitted: 4 February 2000
Revised: 2 June 2000
Accepted: 27 June 2000

References

Boleti, H., E. Karsenti, and I. Vernos. 1996. Xklp2, a novel *Xenopus* centrosomal kinesin-like protein required for centrosome separation during mitosis. *Cell*. 84:49–59.

Chui, K.K., G.C. Rogers, A.M. Kashina, K.P. Wedaman, D.J. Sharp, D.T. Nguyen, and J.M. Scholey. 2000. Roles of two kinesins in sea urchin embryonic cell division. Submitted.

Devereux, J., P. Haeberli, and O. Smithies. 1984. A comprehensive set of sequence analysis programs for the VAX. *Nucleic Acid Res.* 12:387–395.

Echeverri, C.J., B.M. Paschal, K.T. Vaughan, and R.B. Vallee. 1996. Molecular characterization of the 50-kd subunit of dynactin reveals function for the complex in chromosome alignment and spindle organization during mitosis. *J. Cell Biol.* 132:617–633.

Goldstein, L.S.B. 1993. With apologies to Scheherazade - tails of 1001 kinesin motors. *Annu. Rev. Genet.* 27:319–351.

Groigno, L., and M. Whitaker. 1998. An anaphase calcium signal controls chromosome disjunction in early sea urchin embryos. *Cell*. 92:193–204.

Henson, J.H., D.G. Cole, M. Terasaki, D. Rashid, and J.M. Scholey. 1995. Immunolocalization of the heterotrimeric kinesin-related protein KRP((85/95)) in the mitotic apparatus of sea urchin embryos. *Dev. Biol.* 171:182–194.

Hinchcliffe, E., G.O. Cassels, C.L. Rieder, and G. Sluder. 1998. The coordination of centrosome reproduction with nuclear events of the cell cycle in the sea urchin zygote. *J. Cell Biol.* 140:1417–1426.

Holzbaur, E.L.F., and R.B. Vallee. 1994. Dyneins: molecular structure and cellular function. *Annu. Rev. Cell Biol.* 10:339–372.

Hoyt, M.A., and J.R. Geiser. 1996. Genetic analysis of the mitotic spindle. *Annu. Rev. Genet.* 30:7–33.

Karsenti, E., H. Boleti, and I. Vernos. 1996. The role of microtubule dependent motors in centrosome movements and spindle pole organization during mitosis. *Semin. Cell Dev. Biol.* 7:367–378.

Kashina, A.S., G.C. Rogers, and J.M. Scholey. 1997. The *bimC* family of kinesins: essential bipolar mitotic motors driving centrosome separation. *Biochim. Biophys. Acta.* 1357:257–271.

Kiehart, D.P. 1982. Microinjection of echinoderm eggs: apparatus and procedures. *Methods Cell Biol.* 25:13–31.

Lupus, A., M. Van Dyke, and J. Stock. 1991. Predicting coiled coils from protein sequences. *Science.* 252:1162–1164.

Molina, I., S. Baars, J.A. Brill, K.G. Hales, M.T. Fuller, and P. Ripoll. 1997. A chromatin-associated kinesin-related protein required for normal mitotic chromosome segregation in *Drosophila*. *J. Cell Biol.* 139:1361–1371.

Morris, R.L., and J.M. Scholey. 1997. Heterotrimeric kinesin-II is required for the assembly of motile 9+2 cilliary axonemes on sea urchin embryos. *J. Cell Biol.* 138:1009–1022.

Mountain, V., C. Simerly, L. Howard, A. Ando, G. Schatten, and D.A. Compton. 1999. The kinesin-related protein, HSET, opposes the activity of Eg5 and cross-links microtubules in the mammalian mitotic spindle. *J. Cell Biol.* 147:351–366.

Nakagawa, T., Y. Tanaka, E. Matsuoka, S. Kondo, Y. Okada, Y. Noda, Y. Kanai, and N. Hirokawa. 1997. Identification and classification of 16 new kinesin superfamily (KIF) proteins in mouse genome. *Proc. Natl. Acad. Sci. USA*. 94:9654–9659.

Nigg, E.A. 1993. Cellular substrates of $p34^{cdc2}$ and its companion cyclin dependent kinases. *Trends Cell Biol.* 3:296–300.

O'Connell, M.J., P.B. Meluh, M.D. Rose, and N.R. Morris. 1993. Suppression of the *bimC4* mitotic spindle defect by deletion of *klpA*, a gene encoding a *KAR3*-related kinesin-like protein in *Aspergillus nidulans*. *J Cell Biol*. 120: 153–162.

Pidoux, A.L., M. Ledizet, and W.Z. Cande. 1996. Fission yeast pkl1 is a kinesin-related protein involved in mitotic spindle function. *Mol. Biol. Cell*. 7:1639–1655.

Rogers, G.C. 2000. The functional coordination of three different microtubule-based motors in positioning centrosomes during sea urchin embryogenesis. Ph.D. Thesis. University of California. Davis, CA.

Rogers, S., R. Wells, and M. Rechsteiner. 1986. Amino acid sequences common to rapidly degraded proteins: the PEST hypothesis. *Science*. 234:364–368.

Rogers, G.C., C.L. Hart, K.P. Wedaman, and J.M. Scholey. 1999. Identification of Kinesin-C, a calmodulin-binding carboxy-terminal kinesin in animal (*Strongylocentrotus purpuratus*) cells. *J. Mol. Biol.* 294:1–8.

Saunders, W.S., and M.A. Hoyt. 1992. Kinesin-related proteins required for structural integrity of the mitotic spindle. *Cell*. 70:451–458.

Sawin, K.E., K. Leguellec, M. Philippe, and T.J. Mitchison. 1992. Mitotic spindle organization by a plus-end-directed microtubule motor. *Nature*. 359:540–543.

Scholey, J.M. 1998. Functions of motor proteins in echinoderm embryos: an argument in support of antibody inhibition experiments. *Cell Motil. Cytoskel.* 39:257–260.

Sharp, D.J., K.R. Yu, J.C. Sisson, W. Sullivan, and J.M. Scholey. 1999. Antagonistic microtubule-sliding motors position mitotic centrosomes in *Drosophila* early embryos. *Nat. Cell Biol.* 1:51–54.

Sharp, D.J., H.M. Brown, M.K. Kwon, G.C. Rogers, G. Holland, and J.M. Scholey. 2000. Functional coordination of three mitotic motors in *Drosophila* embryos. *Mol. Biol. Cell.* 11:241–253.

Siegel, L., and K. Monty. 1966. Determination of molecular weights and frictional ratios of proteins in impure systems by use of gel filtration and density gradient centrifugation. Application to crude preparations of sulfite and hydroxylamine reductases. *Biochim. Biophys. Acta.* 112:346–362.

Song, H., M. Golovkin, A.S.N. Reddy, S.A. Endow. 1997. *In vitro* motility of AtKCPB, a calmodulin-binding kinesin protein of *Arabidopsis*. *Proc. Natl. Acad. Sci. USA*. 94:322–327.

Starr, D.A., B.C. Williams, T.S. Hays, and M.L. Goldberg. 1998. ZW10 helps to recruit dynactin and dynein to the kinetochore. *J. Cell Biol.* 142:763–774.

Vaisberg, E.A., M.P. Koonce, and J.R. McIntosh. 1993. Cytoplasmic dynein plays a role in mammalian mitotic spindle formation. *J. Cell Biol.* 123:849–858.

Vernos, I., and E. Karsenti. 1995. Chromosomes take the lead in spindle assembly. *Trends Cell Biol.* 5:297–301.

Vernos, I., J. Raats, T. Hirano, J. Heasman, E. Karsenti, and C. Wylie. 1995. Xklp1, a chromosomal *Xenopus* kinesin-like protein essential for spindle organization and chromosome positioning. *Cell*. 81:117–127.

Warrick, H.M., and J.A. Spudich. 1987. Myosin structure and function in cell motility. *Annu. Rev. Cell Biol.* 3:379–421.

Wittmann, T., H. Boleti, C. Antony, E. Karsenti, and I. Vernos. 1998. Localization of the kinesin-like protein Xklp2 to spindle poles requires a leucine zipper, a microtubule-associated protein, and dynein. *J. Cell Biol.* 143:673–685.

Wright, B.D., M. Terasaki, and J.M. Scholey. 1993. Roles of kinesin and kinesin-like proteins in sea urchin embryonic cell division: evaluation using antibody microinjection. *J. Cell Biol.* 123:681–689.

Zamyatnin, A.A. 1972. Protein volume in solution. *Prog. Biophys. Mol. Biol.* 24:107–123.